

X-ray Photoelectron Spectroscopy of Polymers Explored using Poly Methyl Methacrylate

Data Analysis: Neal Fairley

Experimental Data: Pascal Bargiela

Abstract

This article provides an overview of data treatment aimed at understanding the X-ray Photoelectron Spectroscopy of poly methyl methacrylate. Videos detailing data analysis steps provide the technical aspects of the analysis, therefore the text below is designed to supplement videos by providing the context for the material and methods used in the analysis. Videos focus on methodology in CasaXPS rather than explanations of how and why these data treatments are performed. The combination of this article and videos provides a case study of fitting peak models to data. These peak models are constructed using mathematical line shapes to define components of the peak model. Components to peak models are designed to correlate photoemission signal with chemical state, which is achieved by identification of binding energy and relative intensity of photoemission signal that can be attributed to atoms in specific chemical environments. While the primary thrust of this case study is correlating components to chemical state, a technique to achieve this end makes use of linear algebraic concepts to facilitate the construction of a peak model that elucidates the nature of PMMA spectra, as-measured.

Introduction

Polymers are arguably materials that are best suited to analysis by X-ray Photoelectron Spectroscopy (XPS)¹. Primarily, photoemission from carbon results in well-formed, mostly symmetric, bell-shaped intensity distributions about a well-defined mean energy, that responds to bonding between atoms by shifts in energy from the nominal binding-energy of electrons in an atom. The uniform structure of most polymers is ideal for XPS as these mostly conform to the concept of homogeneous materials, a necessary condition for easy quantification of a sample in terms of atomic concentration². Hence, the XPS of polymers offers, through binding energy shifts, chemical state information for atoms and, through area of photoemission distributions, the relative proportions of different chemical state for atoms within a polymer. Further, many polymers are formed from carbon bonded to low atomic number elements. Bonding electrons in polymers rarely exist between carbon and d-orbitals, so complex initial- and final-state energy-multiplicity^{3,4}, observed in metal-oxide photoemission, is less of an issue for the XPS of polymers. Consequently, peak models constructed from components with shapes defined by Voigt-like curves are more plausible, when applied to polymer materials, than the XPS of heavy-metal oxide materials. These considerations all support the use of XPS when studying polymer materials.

The following represents the analysis⁵ of poly methyl methacrylate (PMMA) by XPS. The expected relationship between atoms in PMMA is shown in Figure 1. The XPS of PMMA is a good case study because carbon appears in four distinct chemical states (C- \underline{C} H, C- \underline{C} -C, \underline{C} -O and O- \underline{C} =O), while oxygen in PMMA are examples of single and double bonding of oxygen with carbon. Photoemission from C 1s and O 1s subshells respond to these chemical bonds by shifts in binding energy, that can be identified in XPS data using mathematical modelling of C 1s and O 1s photoemission. Precise numbers of components forming peak models, must follow the chemistry shown in Figure 1. These mathematical models are used to test the hypothesis: the sample is PMMA. By fitting four component-curves in the proportion 1:1:1:2 (measured by area beneath a component-curve) to C 1s, and fitting two component-curves of equal area to O 1s data, the relationships between atoms in Figure 1 are shown to be feasible for a sample under analysis. Despite the apparent simplicity for the analysis as describe thus far, PMMA also provides an example for an aspect of XPS that is sometimes overlooked. That is, XPS measurement causes alteration to the polymer chemistry⁶. If an experiment aimed at understanding the chemistry of PMMA is repeated many times, it becomes apparent that the spectra change with each iteration and these changes reflect an alteration of the material during the measurement process. An experiment of this nature is performed and the analysis of these data is presented below.

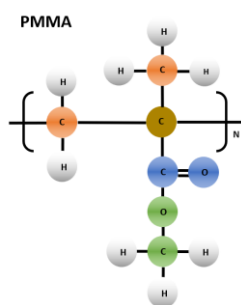


Figure 1. poly methyl methacrylate. Carbon and oxygen atoms are colour coded, where each colour represents a bonding environment for atoms that cause a specific shift in binding energy for C 1s and O 1s photoemission. The number of carbon atoms with the same colour is used to infer similar chemical shifts in energy and therefore photoemission intensity for these five carbon atoms manifests in XPS C 1s spectra in the proportions 1:1:1:2. XPS O 1s spectra similarly show two distinct photoemission peaks due to a double bond O=C and a single bond C-O-C.

Modelling Photoemission using Mathematical Curves

Line shapes for Polymers

Core-level electrons, even for atoms within solid state, are associated with well-defined quantized energy-levels, which when scattered by photons of a precise energy, manifest in energy spectra as counts, distributed about the mean energy, with shapes similar in appearance to Gaussian or Lorentzian functions. Isolated photoemission peaks, in particular s-orbitals, tend to favour a Lorentzian (Eq. A1) distribution of signal about the mean energy. However, after transfer of signal from the sample through the spectrometer, also allowing for the response of the sample to charge compensation, the distribution of signal as measured is often different from a pure Lorentzian. Hence, the line shapes described in the Appendix includes a Voigt function formed by convoluting a Lorentzian with a Gaussian (Eq. A4, Eq. A5). The Gaussian (Eq. A2), when convoluted with a

Lorentzian, models the spectrometer contribution to the apparent photoemission peak shapes. A corollary to these considerations is that, for a given photoemission line, such as C 1s or O 1s, the apparent peak shape differs between instrumental modes (in the form of pass energy and lens modes) and differs between instruments. Thus, while the number of component-curves forming a peak model remains constant and independent of instrumental factors, the line shape for each component may differ due to differences in instrumentation. A Voigt function, which is a special case of the convolution in Eq. A4, represents a class of line shapes. Examples of these Voigt line shapes are shown in Figure 2. The area beneath each curve in the set of Voigt line shapes shown in Figure 2 is identical. However, owing to the change of characteristic shape between a line shape that favours a Gaussian (LA(10)) to a line shape that favours a Lorentzian (LA(90)), the height of the line shape for the same area and FWHM reduces as the m parameter (Eq. A5) increases. Consequentially, components in a peak model defined with different Voigt line shapes have the potential to alter the intensity as measured by components when fitted to data. Thus, in choosing a line shape for a component, the line shape represents a constraint on the possible outcomes when fitting a peak model to data and allows alteration to the relative intensity of components to a peak model obtained by fitting the peak model to data. The subject of line shapes and their influence on peak models constructed to represent the four chemical states of carbon in PMMA is relevant to the outcomes described below.

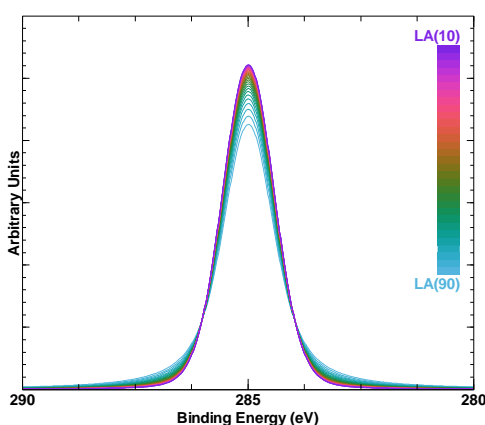


Figure 2. $LA(m)$ line shapes (Eq. A5) generated by varying the line shape parameter m within the interval $[10,90]$. All line shapes are plotted using the same area and the same full width half maximum (FWHM). Note how the height of these line shapes changes as m varies between 10 and 90.

Peak Model Optimisation Constraints

Components to a peak model are a set of line shapes together with parameters that define the energy, the width and intensity of a photoemission peak. Since the physics of the photoemission process dictates that photoemission signal from an atom in a specific chemical environment must take the form of a distribution about a characteristic energy, with a characteristic width and intensity that is in proportion to atoms expected for a given sample, these energy-, width- and intensity-parameters must be restricted during optimisation⁷. These restrictions to component parameters prevent fitting of a peak model to data returning nonphysical values. For example, the peak model in Figure 3, when fitted to C 1s data acquired from a sample presented as PMMA, returns component parameters that are compatible with the expected chemical environments for

carbon in PMMA. Specifically, the proportions for components (measured by area) are in reasonable agreement with the chemistry of PMMA and components are shifted in binding energy as expected for PMMA. By way of contrast, Figure 4 illustrates a peak model, in the absence of any constraints, that yields outcomes for component parameters which fail to return meaningful values for carbon in PMMA. Figure 4 represents a mathematical solution to fitting four unconstrained components in a peak model to the same data in Figure 3, which is of little physical value. The role of parameter constraints in the analysis of XPS data by peak models is highly significant to outcomes.

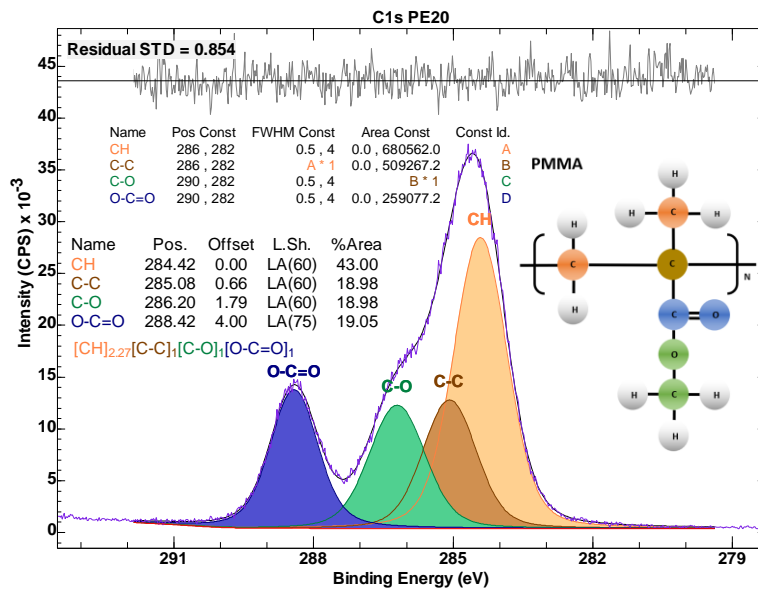


Figure 3. Peak model constructed for PMMA measured using NEXSA G2, pass energy 20. The constraints applied to optimisation parameters are displayed in the top-most table. The constraints of significance to the component intensities and binding energies are the two relational constraints in which the FWHM of the C-C component is forced to be identical to the FWHM of the CH component, and the area of the C-O component is identical to the area of the C-C component. Interval constraints, although defined for all other parameters, in this example, do not play a role in limiting the optimisation adjustments to parameters.

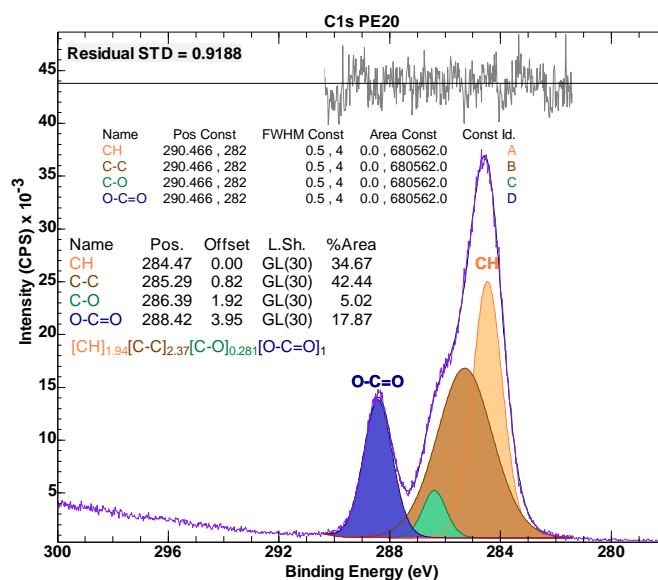


Figure 4. The same data shown in Figure 3 is fitted using a peak model using different line shapes and no relational constraints of the form used in Figure 3. An equal number of four components with line shapes using the legacy line shape GL(30) (Eq. A6) are allowed to adjust within wide interval constraints. When optimisation is applied, the result is a nonphysical outcome, in the sense that, components to the peak model cannot be assigned to chemical state for carbon within PMMA.

Types of Constraints to Optimisation Parameters

Energy, width and intensity parameter-constraints may take one of two forms, namely, interval constraints or relational constraints. Interval constraints limit a parameter from accepting a value that is outside of a range of values. Relational constraints force a parameter value within one component to the value of a second component. Both types of constraints are illustrated in Figure 3, while the peak model in Figure 4 makes use of interval constraints only. The peak model in Figure 4 is effectively unconstrained and, when optimisation selects the best fit for these C 1s PMMA data, the results are of no scientific value. When relational constraints (which are still of a limited nature compared to the freedom afforded to the other optimisation parameters) are applied to the peak model in Figure 3, the constraints provide guidance to the optimisation algorithm that yields four components to the peak model with energy offsets and relative intensities that are consistent with PMMA chemistry. These constraints in Figure 3 are necessary to achieve the result shown, but these constraints presuppose the sample chemistry is that of PMMA. It should be noted that, assuming the sample is PMMA has a greater influence on the design of the peak model in Figure 3 than imposing these relational constraints, namely, the peak model is constructed using four components, only. Every assumption in the form of constraints or the number of components represents a bias introduced into the analysis. When constructing a peak model, if the desire is to gain information about possible chemistry for a sample, the fewer assumptions, the more likely additional information is discerned from fitting the peak model to data. For example, it would be possible to force, through area constraints, the exact stoichiometry of PMMA, however, it is preferable to introduce limited constraints, such as the two relational constraints in Figure 3, on the bases that a peak model with fewer constraints may provide additional information, over and above, demonstrating that PMMA is a feasible chemistry for the sample. For example, the more restrained use of constraints for the peak model in Figure 3, returns four distinct chemical states, three of which are identical in intensity, while the CH component intensity suggests an excess of CH type carbon compared to C-C, C-O and O-C=O environments for carbon. If a more rigid set of constraints are used to force all four components to obey the stoichiometry of PMMA, the only hint that the model is less than perfect would be inferior residual statistics, which are not directly open to interpretation in terms of chemistry.

Modelling Photoemission using Curves from Data

Analysis of polymers by peak models constructed from mathematical line shapes is the most direct and most used method for identifying chemical state. However, simply because a peak model, when optimised to fit data achieves good fitting statistics⁸, this does not prove a perceived sample composition is correct. A case in point is the peak model in Figure 3. The sample is assumed to be PMMA and, in constructing the peak model, it is assumed the spectrum in Figure 3 is entirely due to photoemission from PMMA. The model fits these data with fitting statistics supporting the ability of four components in the peak model to concur with the hypothesis of PMMA as the source for the spectrum. The only hint that signal originating from other than PMMA is the apparent excess of CH

type signal. The expected ratio for PMMA for C 1s photoemission is 2:1:1:1, which is close enough to the results presented in Figure 3 to conclude that PMMA is most likely the composition of the sample. Nonetheless, a lingering doubt that the peak model may be an over simplification is confirmed by extending the experiment to multiple iterations of the same photoemission lines. Figure 5 displays spectra measured from PMMA over ninety experiment cycles recording C 1s, O 1s and valence band spectra. The colour scales used to plot these spectra highlight the evolution in spectra in all three energy intervals. The fact that some polymers are degraded during analysis by XPS is well known. PMMA is one of these polymers that degrade, so that results shown in Figure 3 may suggest that, even for the first iteration of the measurement in the set of iterations in Figure 5, the C 1s spectrum in Figure 3 may be subject to some alteration during the measurement of O 1s or valence band spectra. The degree of change to the initial PMMA material can be assessed by analysis of the data shown in Figure 5 using techniques based in linear algebra. Applying these linear algebraic techniques to spectra in Figure 5 allows an estimate for the rate of degradation. More importantly, linear algebraic techniques also show the extent to which degradation must be accounted for, if a precise peak model for C 1s measured from a pristine PMMA sample is desired. Specifically, an analysis of the data in Figure 5 suggests the need for additional components to a peak model to account for, unavoidable differences in chemistry from the expected chemistry shown in Figure 1.

Applying linear algebraic techniques to data^{9,10} in Figure 5 allows an investigation into how many component-spectra are required to construct a model. The definition of a model differs between a model constructed from mathematical line shapes and a model formed from component-spectra calculated from data. Component-spectra calculated from data are not correlated with chemical bonds, but are the sum of photoemission from ensembles of chemical bonds that can be identified as a phase of a material, for example pure PMMA chemistry as defined by Figure 1. A model formed from component-spectra are fitted to data in a linear least squares sense and must fit to each spectrum in the original data set with equally good precision. The fitting procedure is therefore very rigid and unforgiving in the sense that the component-spectra must include all the shape information required to fit the original spectra without allowing for energy shifts or broadening of features. Peak models constructed from components with mathematical line shapes and fitting parameters are open to shifts and changes in width to photoemission distributions, which are determined by nonlinear optimisation algorithms, are more flexible and each component to the peak model is interpreted as a specific chemical state in a material. Therefore, despite gaining information about spectra through constructing component-spectra-from-data, peak models in the image of Figure 3 are essential to interpreting the meaning for component-spectra calculated from data. These two approaches to XPS data analysis are therefore complementary rather than separate paths to a solution.

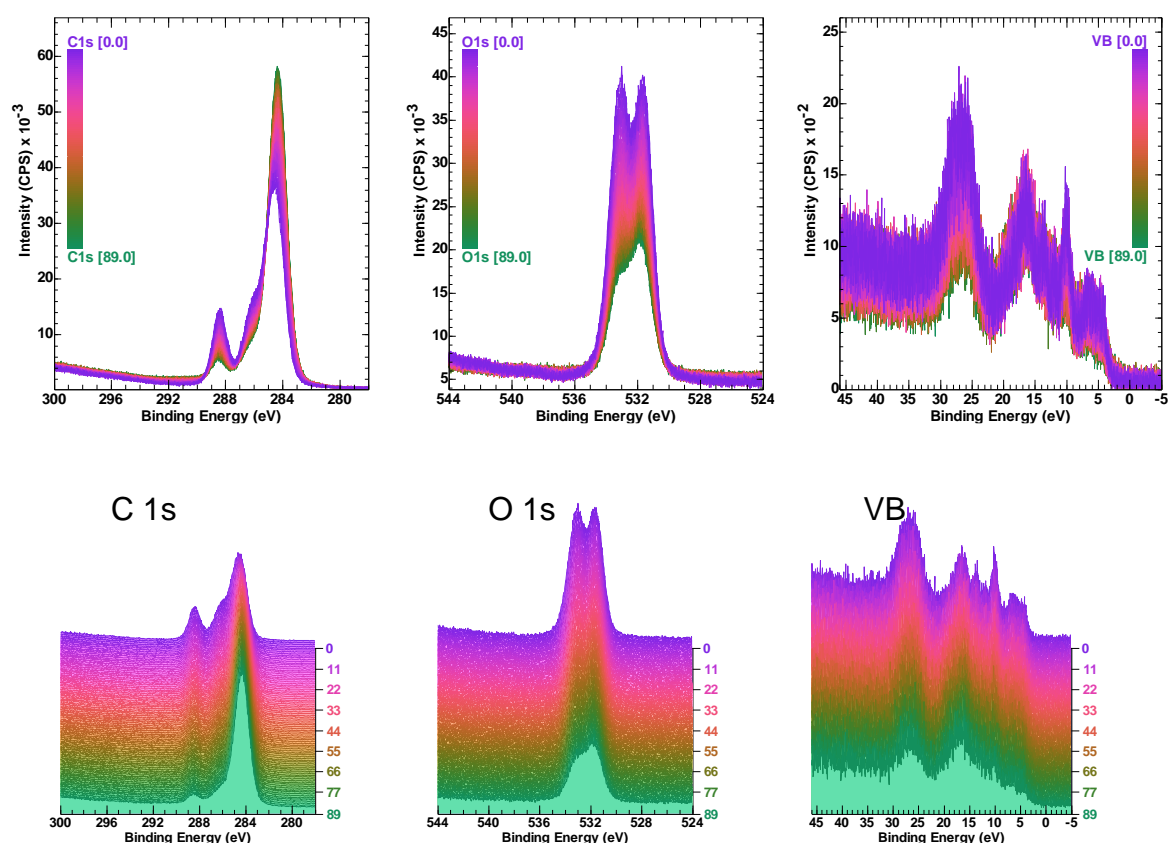


Figure 5. XPS of PMMA performed over 90 iteration cycles in which C 1s, O 1s and valence band spectra are repetitively measured without altering the analysis position or any other intervention that would explain alterations in spectra as shown.

Principal Component Analysis

Given data of the form presented in Figure 5, the first problem is to quantify the number of component-spectra that would be required to represent spectroscopic shapes in these data. It is the role of Principal Component Analysis (PCA) to furnish information of this nature. PCA does not compute from spectra spectroscopic shapes. Rather, spectra are transformed into mathematically equivalent abstract spectra, in the sense that each spectrum in the original data set may be specified using a linear combination of the abstract spectra. The purpose of computing these abstract spectra is to count the number of abstract spectra that include sufficient variation in intensity to be considered different from noise. The number of abstract spectra that differ from noise is an indication of how many component-spectra should be sought. Abstract-spectra, limited in number to the abstract-spectra distinct from noise, serve as inputs to an operation aimed at reducing the influence of noise on the spectra in Figure 5. Replacing each spectrum in Figure 5 by a linear least square fit of these chosen abstract-spectra provides spectroscopic data with reduced noise characteristics.

Calculating Component-Spectra from Difference Spectra

The objective in forming difference spectra, is to partially remove from one spectrum, a contribution of the other spectrum. By forming a sequence of difference spectra, that offer incremental changes in the contribution of one spectrum to the other, a visual representation of these changes in spectra are made available for inspection. Component-spectra are selected from a list of difference spectra.

The success or failure of calculating component-spectra depends on the quality and rate of evolution within the data set. While in certain circumstances, identifying component-spectra that correspond to specific chemical states for an atom, it is often the case, as demonstrated by the analysis of iteratively measured C 1s spectra from PMMA, it is not possible to separate the chemical states of carbon within PMMA, but it is possible to identify PMMA as a distinct material and a material that is created from PMMA during the measurement process.

Using C 1s spectra shown in Figure 5 only, it is possible to compute difference-spectra using subsets of these C 1s spectra (Figure 6). A subset is selected to include a sufficient number-of-spectra, that were measured sequentially, to permit PCA to demonstrate that the subset of spectra belongs to a two-dimensional subspace and therefore capable of approximation by two component-spectra only. Using the first two most significant abstract-spectra, the subset of spectra are replaced by fitting, to each spectrum, these two abstract-spectra, then replacing the original spectra by these least squares fit of abstract-spectra to data. Assuming the evolution in spectral shapes is due to XPS of PMMA and therefore a continuous incremental change, difference-spectra are formed from the first and last noise-reduced approximate spectra that allows an estimate for both spectra from PMMA and the degraded PMMA to be obtained. Performing this calculation using different subsets, selected over different periods within the experiment, furnishes alternative perspectives for spectra from PMMA and the degraded PMMA. Iterations in analysis steps making use of subsets from the initial phase of the experiment and the latter phase demonstrates that, at all measurement iterations, PMMA is present and, more importantly, it is feasible that the degraded form of PMMA is also present in all spectra, including the first measurement performed on PMMA. Figure 7a shows two component-spectra calculated through analysis of data shown in Figure 6. Note how, for the component-spectrum labelled PMMA in Figure 7a, by applying the peak model in Figure 3, optimisation returns the expected stoichiometry of PMMA defined by Figure 1. The hypothesis for modelling the spectrum in Figure 3 is therefore, that the peak model in Figure 3 requires additional components, which might take the form of the peak model shown in Figure 7b. These additional components in Figure 7b are accounting for degradation of PMMA, which was not considered when the peak model in Figure 3 was conceived.

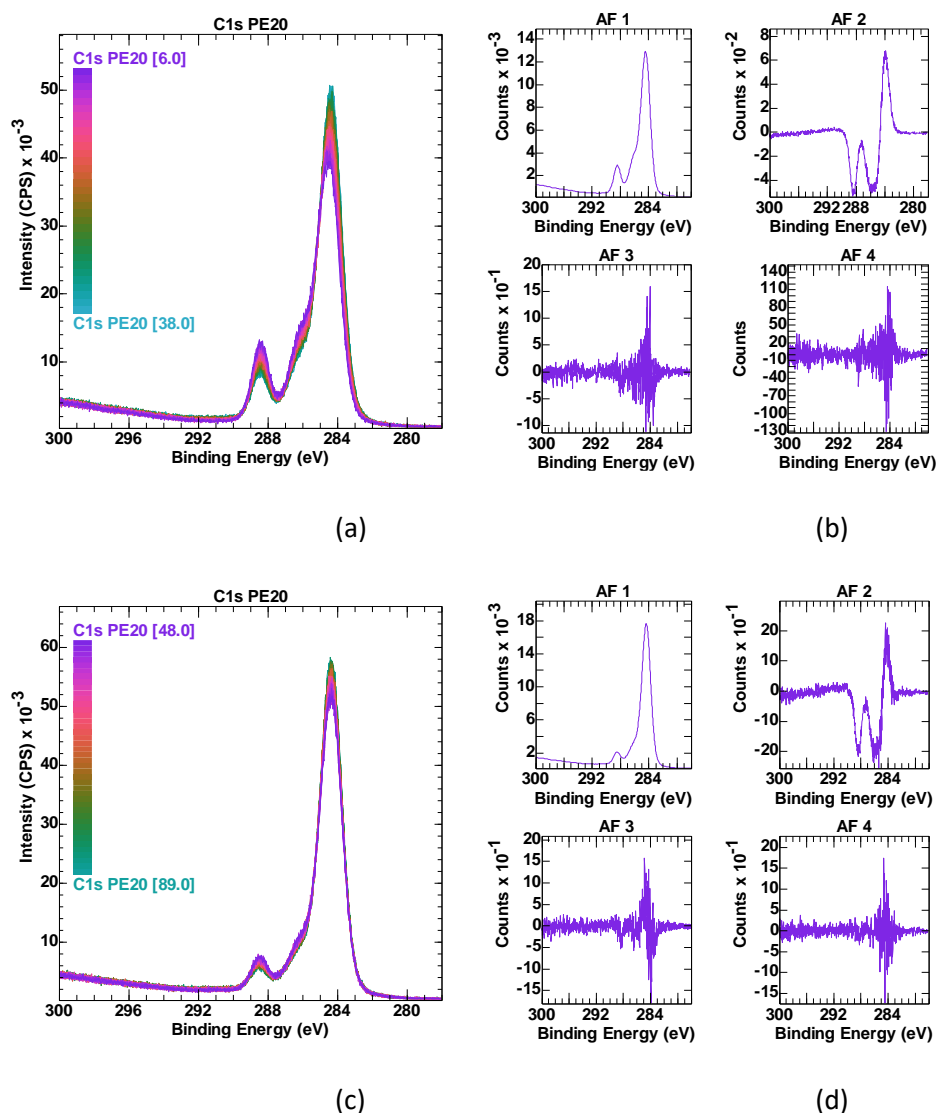


Figure 6. Examples of two subsets of C 1s spectra from data shown in Figure 5 used to investigate component-spectra for PMMA and degraded PMMA. Spectra in (a) are a subset measured during iterations 6 to 38. Spectra in (c) are a subset measured during iterations 48 to 89. Abstract-spectra computed from the spectra in (a) and (c) are presented in (b) and (d), respectively.

Linear Least Square Optimisation

The peak models using mathematical components in Figure 7a are fitted to data using nonlinear optimisation. These two component spectra shown in Figure 7a are calculated from the data in Figure 5. The spectrum in Figure 7b is the same data shown in Figure 3, but in Figure 7b, the components are added to these C 1s data by fitting the component-spectra in Figure 7a to the spectrum in Figure 7b using linear least square optimisation. Since the fit of these two component-spectra to the data in Figure 7b scales the intensity of these two component-spectra in Figure 7a, it is a simple matter to scale the components to each peak model in Figure 7a and add these scaled components to form the peak model shown in Figure 7b. No nonlinear optimisation is directly

applied to fit these eight components to the data in Figure 7b. Consequently, there is no need to alter the optimisation parameter constraints used to fit the two peak models separately to the two component-spectra in Figure 7a.

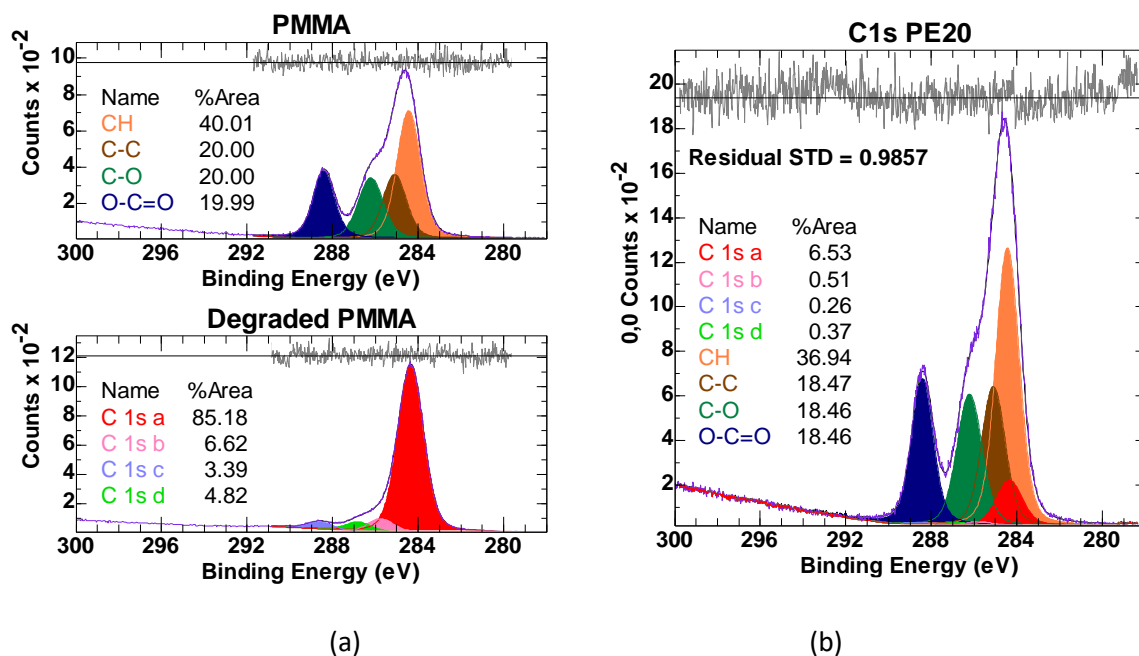


Figure 7. (a) Component-spectra calculated from data shown in Figure 6, fitted with two peak models, one using components correlated with photoemission from pure PMMA and the second fitted using four uncorrelated components corresponding to degraded PMMA. (b) As-received surface of PMMA sample measured by XPS fitted with a peak model constructed from the components shown in (a). Construction steps include forming a linear least square fit of the two component spectra in (a) to the data in Figure 3. The peak models applied to component-spectra in (a) are scaled and applied to the data in (b), resulting in a peak model involving eight component peaks, four of which are positively assigned as PMMA photoemission.

The mathematics of linear least square optimisation is included in the Appendix. A further example of a spectrum fitted by linear least square optimisation is included in Figure A1. The same fitting procedure used to construct the fit to data shown in Figure A1, is used to fit the data in Figure 7b. The scale factors computed for the spectrum in Figure 7b, allow two peak models shown in Figure 7a, fitted to the $f_1(x)$ and $f_2(x)$ as defined in Figure A1, to be transferred to the spectrum in Figure 7b. The fit is therefore achieved without the use of nonlinear optimisation adjusting the peak model formed from these eight components. That is, linear least square fitting of component-spectra allows the construction of the peak model containing eight components shown in Figure 7b without the need for additional constraints between these eight components.

Appendix

Mathematical Line Shapes

The underlying functional forms used to construct mathematical line shapes are Lorentzian (Eq. A1) and Gaussian (Eq. A2). New line shapes are formed from these two functional forms Eq. A1 and Eq. A2, in the case of Eq. A5 by means of the convolution defined in Eq. A4.

$$\text{Lorentzian: } l(x) = \frac{1}{1+4x^2} \quad (\text{A1})$$

$$\text{Gaussian: } g(x) = e^{-4\ln 2 x^2} \quad (\text{A2})$$

Voigt line shapes are defined from Lorentzian and Gaussian functions via the special case of a generalized Lorentzian (Eq. A3) and the convolution integral in Eq. A4

$$\text{Generalised Lorentzian: } l_g(x; \alpha, \beta) = \begin{cases} [l(x)]^\alpha & x \leq 0 \\ [l(x)]^\beta & x > 0 \end{cases} \quad (\text{A3})$$

$$\text{Lineshape: } LA(x; \alpha, \beta, n) = N \int_{-\infty}^{\infty} l_g(\tau; \alpha, \beta) g(x - \tau; f_G(n)) d\tau \quad (\text{A4})$$

The symmetric line shape $LA(x, m)$ (Eq. A5), specified in CasaXPS by the string $LA(m)$, is constructed from the definition for $LA(x; \alpha, \beta, n)$ and the maximum allowed value n (1401) defining the width for the Gaussian term in the LA convolution integral in Eq. A4.

$$LA(x, m) = LA\left(x; 1, 1, \left(1401 - \left(\frac{m}{100}\right) 1401\right)\right) \quad (\text{A5})$$

The Gaussian-Lorentzian product (GL(m)) pseudo-Voigt peak shape, Eq. A6, is formed from the product of Gaussian and Lorentzian functions (Eq. A2 and Eq. A1),

$$GL(x, m) = \begin{cases} l\left(\frac{x}{f_L}\right) \times g\left(\frac{x}{f_G}\right) & \dots \quad 0 < m < 100 \\ l(x) & \dots \quad m = 100 \\ g(x) & \dots \quad m = 0 \end{cases} \quad (\text{A6})$$

where the FWHM for each function, f_L and f_G , Eq. A6, vary according to the parameter, $m \in (0, 100)$, as follows:

$$f_L^2 = \frac{1}{\frac{m}{100}} \quad \text{and} \quad f_G^2 = \frac{1}{1 - \frac{m}{100}}. \quad \text{The } m \text{ parameter in } GL(m) \text{ therefore alters the relative FWHM of the}$$

Gaussian and Lorentzian functions (in an attempt) to simulate the behaviour of a true Voigt line shape.

Linear Least Square Optimisation

Given a set of m linearly independent functions $\{f_1(x), f_2(x), f_3(x), \dots, f_m(x)\}$ a function $y(x)$, centred at the origin, can be defined by Eq. A7.

$$y(x) = c_1 f_1(x) + c_2 f_2(x) + c_3 f_3(x) + \dots + c_m f_m(x) \quad (\text{A7})$$

Where, $c_1, c_2, c_3, \dots, c_m$ are coefficients that may be chosen during optimisation so that $y(x)$ reproduces (approximates) a function defined by spectral data. The function $y(x)$ is a linear combination of the functions $\{f_1(x), f_2(x), f_3(x), \dots, f_m(x)\}$. If we use the vector notation, in spectroscopic terms these functional forms are intensities measured at a set of energies $\{x_1, x_2, x_3, \dots, x_n\}$, then component-spectra are written as a vector in the form $\mathbf{v}_j = (f_j(x_1), f_j(x_2), f_j(x_3), \dots, f_j(x_n))$ and spectra, with intensity in data bin i with energy x_i defined by $d(x_i)$, yields a vector $\mathbf{d} = (d(x_1), d(x_2), d(x_3), \dots, d(x_n))$. Given the vectors \mathbf{v}_j , a matrix can be defined in terms of these component-spectra in the form of vectors $\mathbf{A} = [\mathbf{v}_1, \mathbf{v}_2, \mathbf{v}_3, \dots, \mathbf{v}_m]$. Linear algebra now provides the necessary means to compute $y(x)$ that best fits the data vector \mathbf{d} as follows.

$$\mathbf{c} = (\mathbf{A}^T \mathbf{A})^{-1} \mathbf{A}^T \mathbf{d} \quad (\text{A8}),$$

Where $\mathbf{c} = (c_1, c_2, c_3, \dots, c_m)$ are the coefficients in A7. An example of a spectrum from Figure 5 fitted with the two component-spectra in Figure 7, is used to illustrate the result of constructing Eq. A7 making use of two functions $f_1(x)$ and $f_2(x)$, then computing two coefficients in Eq. A7, through Eq. A8, resulting in a fit of $f_1(x)$ and $f_2(x)$ to the spectrum.

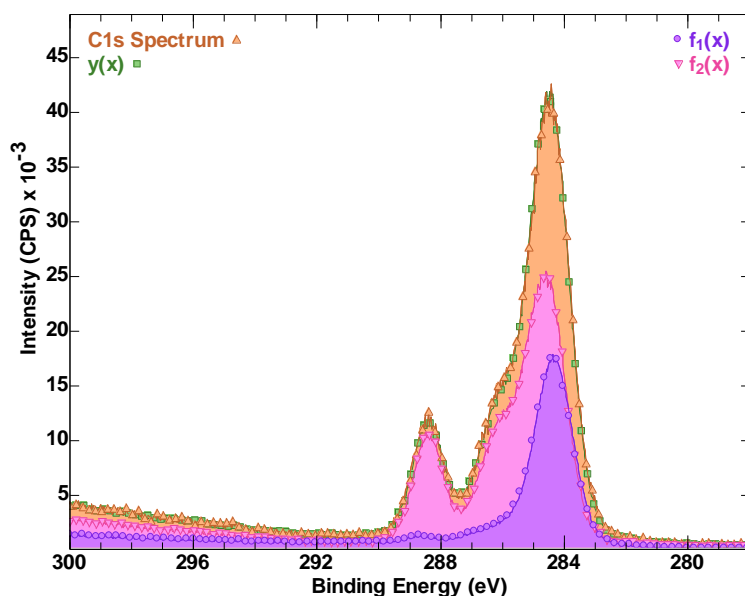
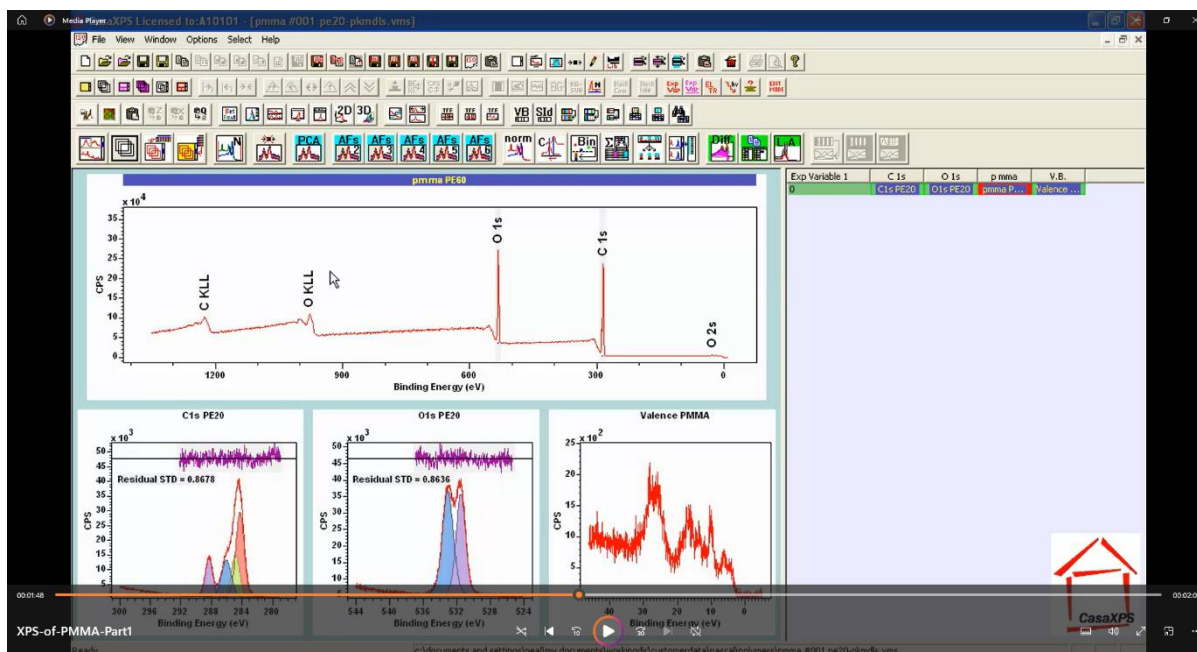


Figure A1. An example of a fit of two component-spectra to a spectrum from the data set shown in Figure 5. The component-spectra are labelled $f_1(x)$ and $f_2(x)$, but correspond to spectra assigned to degraded PMMA and PMMA, respectively. The relationship depicted in this figure is the linear least square fit of these two component-spectra to data formulated using Eq. A7 and calculated using equation A8, subject to nonnegative constraints for the coordinate of the vector \mathbf{c} .

Videos

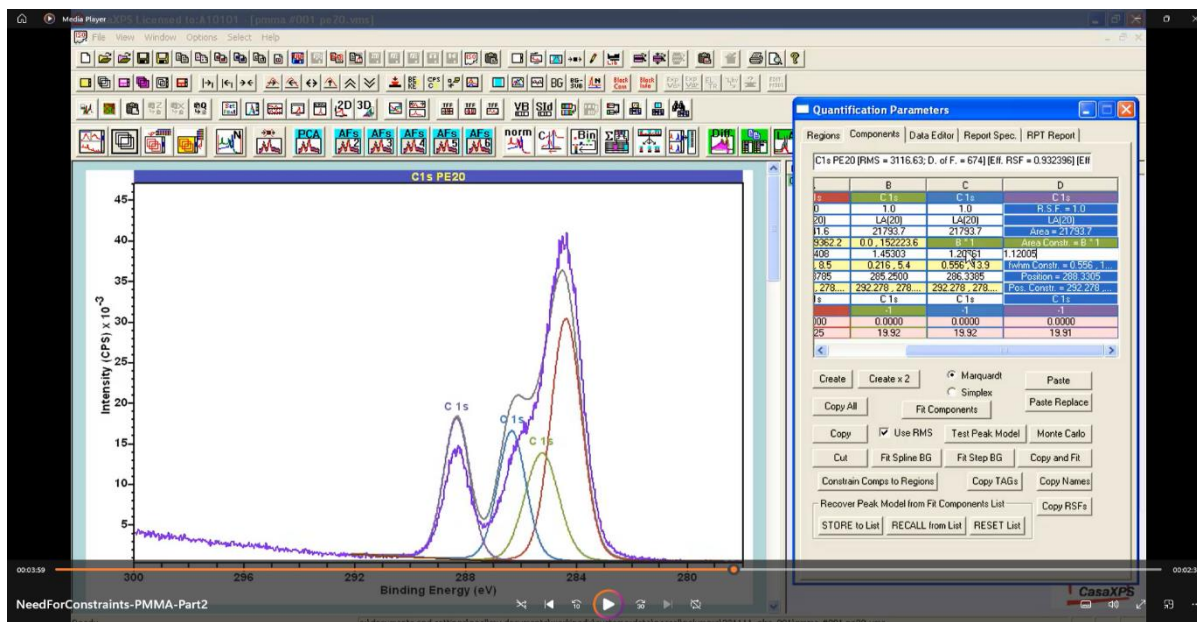
Five videos that illustrate the software features used to construct the results presented above. To start mp4 videos, left-click on the image of the video.

XPS of PMMA: Introduction



The relationship between a peak model, constructed from mathematically defined component peaks, and chemistry of a sample is illustrated using the XPS of PMMA (Figure 1).

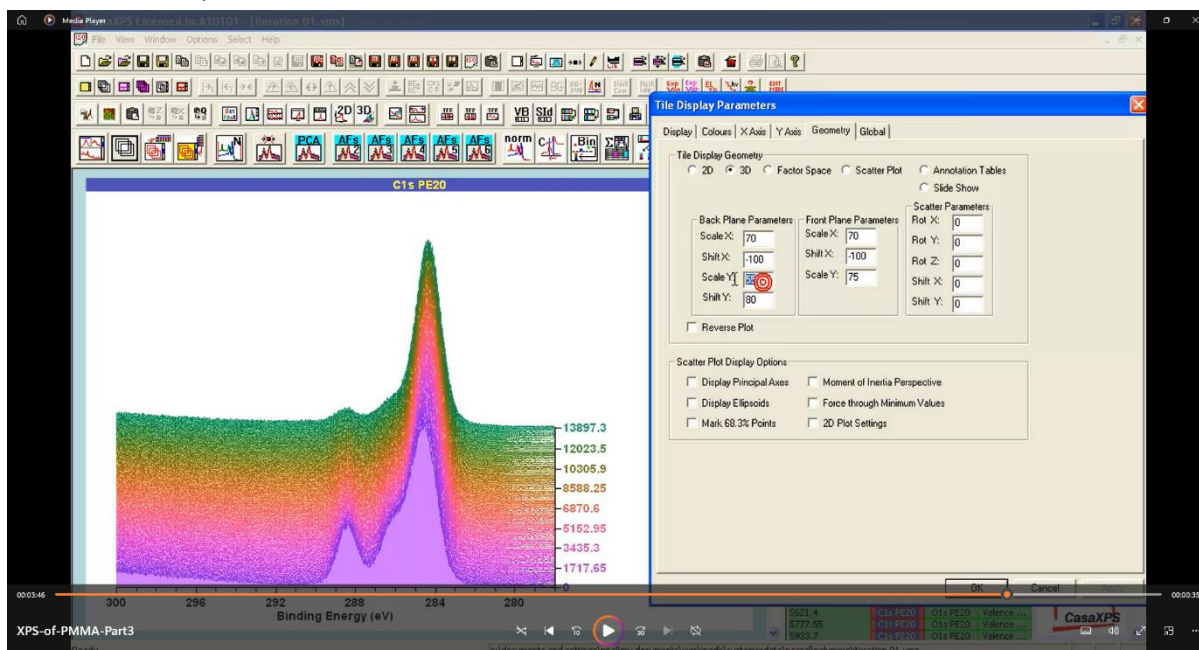
Peak Models and the Need for Constraints



The importance and influence of constraints to optimisation parameters are illustrated in this video. Relational constraints are added to four components forming a peak model for

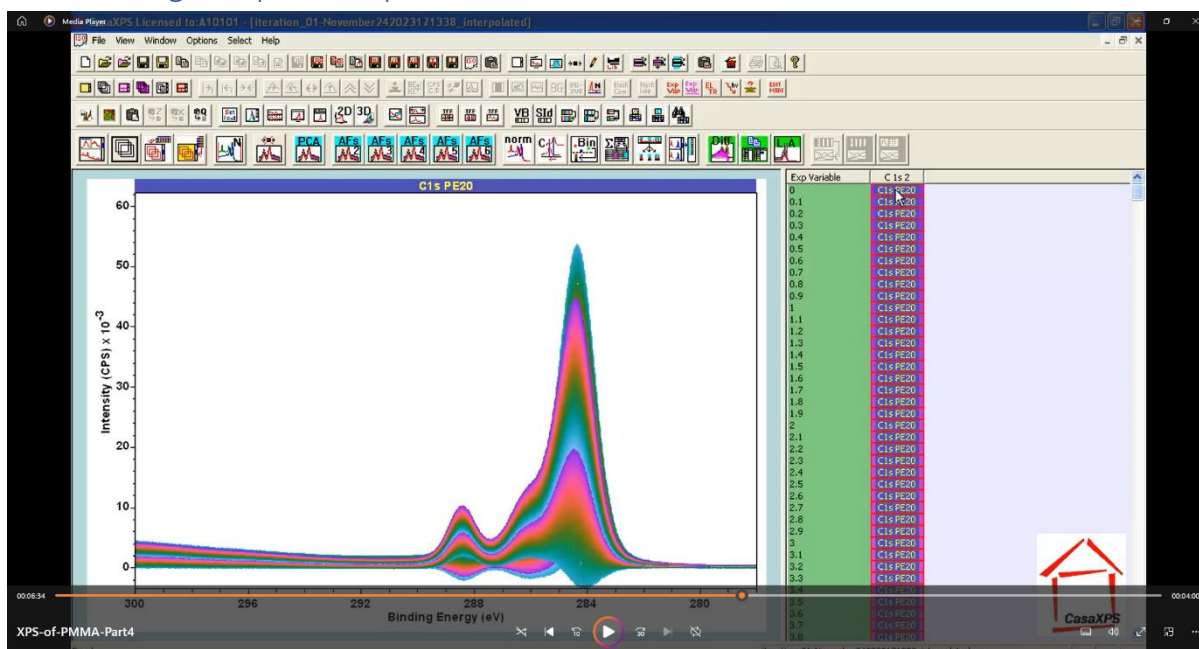
PMMA that illustrate how these types of constraints are used to improve the correlation between component parameters and chemical state information for carbon in PMMA.

Iterations of Spectra from PMMA



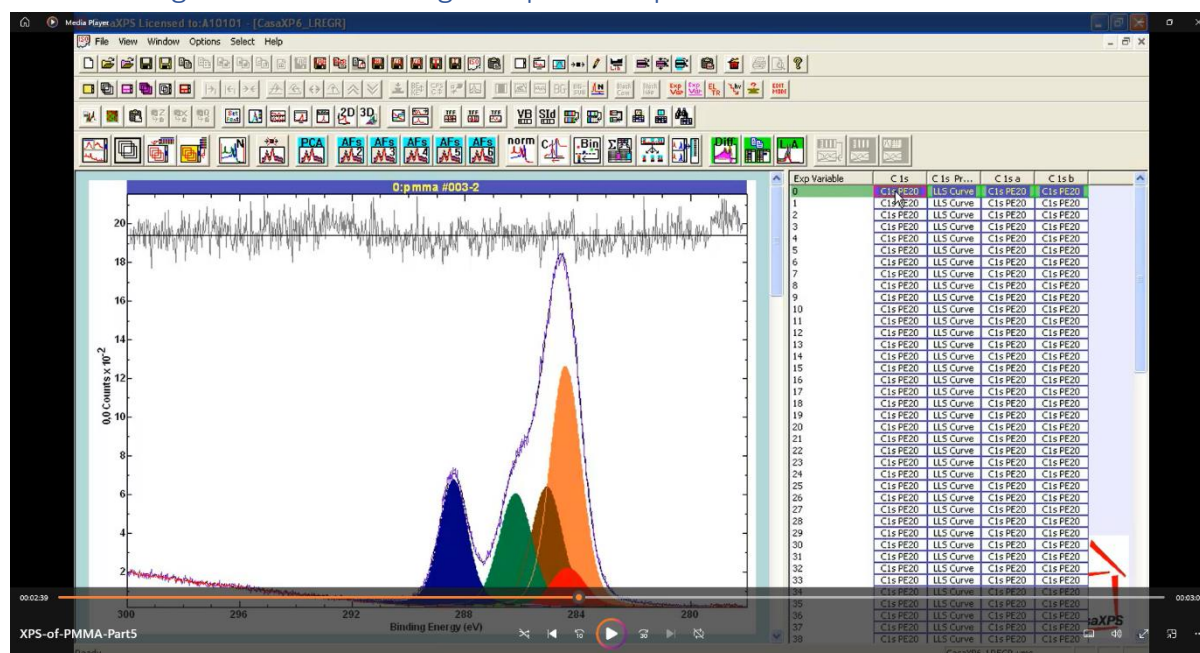
In this video, the experiment consisting of iterations of C 1s, O 1s and valence band spectra are reviewed and display options used to construct Figure 5 are illustrated.

Constructing Component-Spectra



C 1s Data in Figure 5 are processed within this video, the result of which are two component-spectra representing degraded PMMA and PMMA. These component-spectra are illustrated in Figure 7.

Constructing Peak Models using Component-Spectra



The peak model shown in Figure 7b is constructed from the two peak models in Figure 7a.

References

- [1] Briggs, David, and Graham Beamson. "Primary and secondary oxygen-induced C1s binding energy shifts in x-ray photoelectron spectroscopy of polymers." *Analytical chemistry* 64.15 (1992): 1729-1736.
- [2] Fernandez, Vincent, Neal Fairley, and Jonas Baltrusaitis. "Surface analysis insight note: Synthetic line shapes, integration regions and relative sensitivity factors." *Surface and Interface Analysis* 55.1 (2023): 3-9.
- [3] Baltrusaitis, Jonas, et al. "Generalized molybdenum oxide surface chemical state XPS determination via informed amorphous sample model." *Applied Surface Science* 326 (2015): 151-161.
- [4] Morgan, David J. "Photoelectron spectroscopy of ceria: Reduction, quantification and the myth of the vacancy peak in XPS analysis." *Surface and Interface Analysis* 55.11 (2023): 845-850.
- [5] Fairley, Neal, et al. "Systematic and collaborative approach to problem solving using X-ray photoelectron spectroscopy." *Applied Surface Science Advances* 5 (2021): 100112.
- [6] Morgan, David J., and Sharukaa Uthayasekaran. "Revisiting degradation in the XPS analysis of polymers." *Surface and Interface Analysis* 55.6-7 (2023): 556-563.
- [7] Major, George H., et al. "Guide to XPS data analysis: Applying appropriate constraints to synthetic peaks in XPS peak fitting." *Journal of Vacuum Science & Technology A* 40.6 (2022).
- [8] Fairley, Neal, et al. "Practical guide to understanding goodness-of-fit metrics used in chemical state modeling of x-ray photoelectron spectroscopy data by synthetic line shapes using nylon as an example." *Journal of Vacuum Science & Technology A* 41.1 (2023).
- [9] Fairley, Neal, et al. "Principal Component Analysis (PCA) unravels spectral components present in XPS spectra of complex oxide films on iron foil." *Applied Surface Science Advances* 17 (2023): 100447.

[10] Fernandez, Vincent, et al. "Combining PCA and nonlinear fitting of peak models to re-evaluate C 1s XPS spectrum of cellulose." *Applied Surface Science* 614 (2023): 156182.